LBL-27596
OM-271

Presented at the SPIE Optical and Optoelectronic Applied Science and Engineering Conference, San Diego, CA, August 10-11, 1989, and Published in SPIE Volume 1149, Optical Materials Technology for Energy Efficiency and Solar Energy Conversion VIII.

Electron Microscopy and Electrochemistry of Nickel Oxide Films for Electrochromic Devices Produced by Different Techniques

Carl M. Lampert and R'Sue Caron-Popowich
Windows and Daylighting Group
Applied Science Division
Lawrence Berkeley Laboratory
1 Cyclotron Road
Berkeley, California

September 1989

This work was supported by the Assistant Secretary for Conservation and Renewable Energy, Office of Solar Heat Technologies, Solar Buildings Division, of the U.S. Department of Energy under Contract No. DE-AC03-76SF00098.

ELECTRON MICROSCOPY AND ELECTROCHEMISTRY OF NICKEL OXIDE FILMS FOR ELECTROCHROMIC DEVICES PRODUCED BY DIFFERENT TECHNIQUES

Carl M. Lampert and R'Sue Caron-Popowich

Applied Science Division, 1 Cyclotron Rd. (MS 62-203)
Lawrence Berkeley Laboratory, Berkeley, CA 94720 USA

ABSTRACT

In this study we report on our investigation of the microstructure of nickel oxide films produced by e-beam evaporation, sol-gel deposition, and sputtering techniques. We give characteristic cyclic voltammetry, current-voltage relationships, and optical transmission data for films made by each technique. Data is shown for electrodes, both uncycled and cycled, for 17-20 hrs. We found all samples have at least one phase corresponding to cubic nickel oxide (NaCl structure). Other phases, such as nickel hydroxide, may exist but are not immediately identifiable. The stucture of the films ranges from fine polycrystalline to amorphous and varies over the surface of the sample. Films that were cycled for 17–20 hours all tended to have improved transmittance, as high as a 20% change. The highest transmission range from bleached to colored was for the evaporated films, which showed ΔT=60%. The sol-gel films showed a large residual coloration in the bleached state after cycling (about a 40% decline was noted). Overall, after cycling the films appeared to be slightly more crystalline. In all films, after cycling there were increases in the coloration and bleaching current. Also, peak shifts were noted after cycling; the coloration peak tended to shift to higher and the bleaching peak shifted to lower potentials. The overall coloration efficiency (550 nm) for these films ranged from 26-36 cm^2/C.

1. INTRODUCTION

There is growing interest in the development of electrochromic devices for a variety of applications including architectural and automotive glazings.[1-3] Over the last few years, interest in electrochromic nickel oxide has grown, although very little has been reported about the microstructure of this material.[4] There have been substantial X-ray, Raman, and Infrared Spectroscopy studies on the properties of nickel and nickel oxide for battery electrodes.[5] In this study we investigate the issues of (1) differences in films prepared by different techniques, (2) whether oxide films convert to hydroxide after cycling, as determined by electron microscopy, and (3) the effect of cycling on the electrical and optical performance of nickel oxide films.

Before we discuss our findings it is important to cover prior related work on this complicated material. Prior work using cyclic voltammetry[6] and nuclear reaction analysis[7-9] has shown the coloration reaction to be $Ni(OH)_2 \leftrightarrow NiOOH + H^+ + e^-$ with the proton as the dominant ion for coloration. Our previously reported in-situ Fourier Transform Infrared analysis,[10-11] and investigations of others,[12] support the formation of $Ni(OH)_2$ and NiOOH. Other studies[13-19] support reactions involving different nickel oxide species and the hydroxyl ion as the dominant ion. Our work has shown clearly that the reversible process between bleached and colored states involves diffusion of the proton into the film, with the hydroxyl ion playing an important role in the reaction mechanism as verified from in-situ FTIR spectroscopy.[10]

Probably the most revealing indirect microstructural study on the oxidized nickel electrode was done using angle-resolved infrared spectroelectrochemistry.[20] This technique revealed the surface to be an open layer of beta-$Ni(OH)_2$ and hydroxyl groups with free water, under which there is a compact layer of alpha-$Ni(OH)_2$ and bound water layers. As the electrode is oxidized or switched to the colored state, the film transforms to an open surface layer of beta-NiOOH with free water over a compact layer of gamma-NiOOH and bound water.

2. EXPERIMENTAL PROCEDURES

Nickel oxide electrochromic films prepared in three different ways were examined in these experiments by transmission electron microscopy (TEM). Samples were prepared by e-beam vacuum evaporation from nickel oxide, sol-gel deposition followed by a heat treatment, or reactive d.c. sputtering from a nickel target. The samples show representative films but are not optimized in their properties for any given deposition technique. To make electrodes, all films were deposited onto highly doped indium tin oxide (ITO)-coated glass substrates with sheet resistance of about 9 Ω/sq. The ITO-coated glass substrate was 1.4 mm thick and had 83% transmittance at 550 nm. The NiO_x film thicknesses were about 100 nm, measured by a Dektak profilometer. The active electrode area is 3.15 cm^2. For electrochemical and optical measurements, the electrodes were cycled in 1.0 N KOH using a custom computer-controlled potentiostat-spectrophotometer combination. All measurements were made relative to air. Each sample was cycled from 17-20 hours to about 200 cycles. Measurements reported here include initial and final characteristics. The characteristics measured include dynamic voltage, current density, voltammetry, transmittance at 550 nm, and transmittance-voltage relationships. The wavelength of 550 nm was used because it represents the peak of the photopic (human eye response) spectrum. Specimens for TEM were prepared by removing the films with a scalpel. The films were placed on a copper grid that had been covered with a holey carbon film. Silicon particles added to each specimen were used for calibration of each diffraction pattern. These specimens were examined in a Philips 400 electron microscope operated at 100 kV. Energy Dispersive X-ray Spectroscopy (EDS) was done using a Kevex X-ray detector mounted on the microscope.

3. RESULTS AND DISCUSSION

3.1 Evaporated Films

The characteristic voltammetry (-0.5 to 0.6 mV) for an evaporated film is shown in Figure 1. Both the initial and final characteristics are shown in dotted and solid lines, respectively. This convention is used throughout the paper. The final characteristics are obtained after cycling application of a square wave potential of -0.5 to 0.5 V for 18 hours, covering about 200 cycles. Both the coloration and bleaching peak increase in size after cycling. The coloration peak shifts from about 450 mV to 500mV, while the bleaching peak shifts from about 200 mV to 50 mV after cycling. A change in transmittance range is noted after cycling, as shown in Figure 2. The bleached to colored transmittance (550 nm) range is from 82-43% for uncycled films compared to 84-23% for cycled films. This represents a ΔT of 61%, which is comparable to films made by anodic deposition. Our best films by anodic deposition (120 nm) have shown ΔT of 65% at 550 nm.[11] A characteristic time-voltage/current/transmittance plot for an evaporated film is shown in Figure 3. Both inital and final data are shown as dotted and solid lines, respectively. The monochromatic coloration efficiency (550 nm) is 30 cm^2/C initially and declines to 26 cm^2/C after cycling. The reason for this change is that the charge capacity has increased at a faster rate than the increase in optical density. However, the peak coloration current density has remained the same at about 3 mA/cm^2.

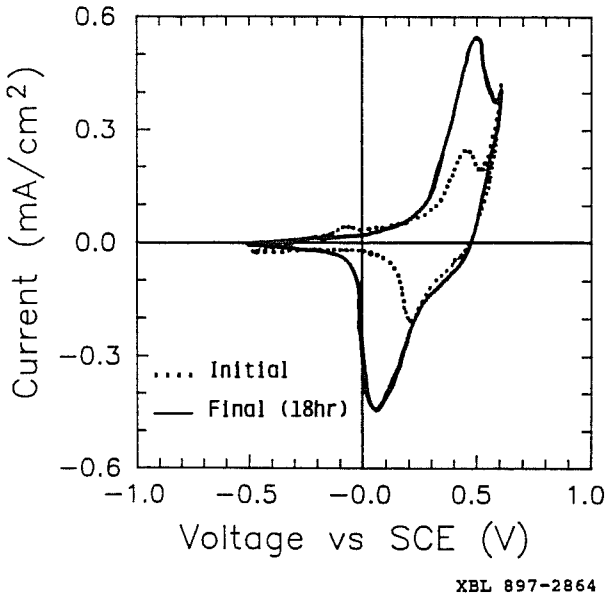

Figure 1. Voltammetry of electrochromic nickel oxide prepared by evaporation. Shown are cycled and uncycled data. The scan rate is 6 mV/s.

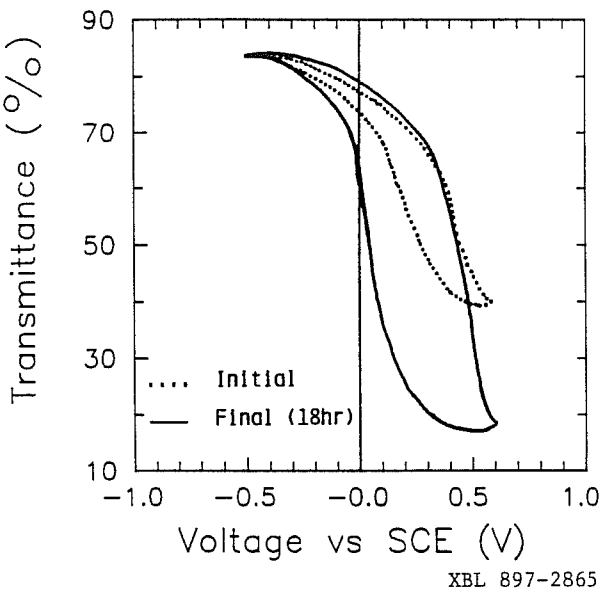

Figure 2. Transmittance (550 nm) versus voltage relationship for electrochromic nickel oxide prepared by evaporation. Shown are cycled and uncycled data.

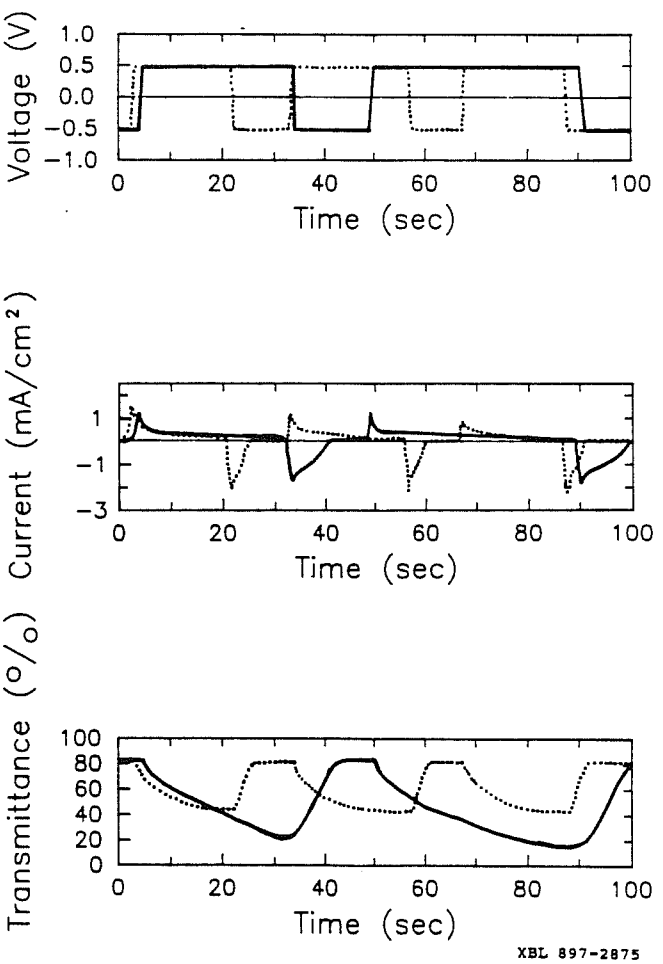

Figure 3. Time-Voltage/Current/Transmittance (550 nm) relationships for evaporated electrochromic nickel oxide.

Transmission electron microscopy (TEM) bright field images and accompanying selected area electron diffraction patterns (SAD) for the evaporated film are shown in Figures 4 A-B. Although the image in Figure 4B shows more bending and breakage, probably from TEM specimen preparation, the main features of the two images are the same. Both have small-grained (25-75 nm) polycrystalline character. The SAD's are also similar. Both index as the cubic phase NiO (a = 0. 4177 nm), (NaCl structure). In our work on anodically deposited nickel oxide we found a similar structure, although the films had a more particulate morphology.[4] The spotted nature of the rings in Figure 4A indicates a higher degree of crystallinity or a larger crystal size than in Figure 4B. All regions of the specimen are represented by either of these figures. Elemental analysis done by energy dispersive X-ray analysis (EDS) verified that the film contained nickel. Unfortunately, oxygen is too light an element to be detected by this method, so nickel to oxygen ratios could not be obtained. In the diffraction patterns no identifiable rings of the nickel hydroxide phase were found. There is the possibility but it is not strongly represented here. This phase may not be stable outside the environment of the switching device and may be especially unstable in the microscope vacuum of 10^{-7} torr. Nickel hydroxide could be present as an amorphous phase or a surface coating with a low volume fraction compared to the bulk nickel oxide layer. If this were the case, detection by SAD would be unlikely. Bright field images of the nickel oxide film after cycling are shown in Figures 5A-B. Both these figures show typical regions of fine polycrystalline cubic nickel oxide. Some preferential orientation can be seen in the SAD in Figure 5B. There also appears to be a larger average grain size compared to the uncycled films, although the difference is difficult to quantify.

3.2 Sol-gel Deposited Films

The voltammetry (-0.5 to 0.6 mV) for a sol-gel deposited film is shown in Figure 6. Both the initial and final characteristics are shown in dotted and solid lines, respectively. The final characteristics are obtained after cycling application of a square wave potential of -0.5 to 0.5 V for 20 hours, covering about 200 cycles. Both the coloration and bleaching peak increase in size after cycling. The coloration peak shifts from about 450 mV to 500 mV, while the bleaching peak shifts from about 250 mV to 150 mV after cycling. This is somewhat similar to the character of the evaporated film. A change in transmittance range is noted after cycling, as shown in Figure 7. The bleached to colored transmittance (550 nm) ranges from 82-63% for uncycled films compared to 43-14% for cycled films. These films show strong residual coloration after cycling—a decline in bleached transmittance of 39%. This represents an initial ΔT of 19% and final value of 29%. A characteristic time-voltage/current/ transmittance plot for a sol-gel film is shown in Figure 8. Both initial and final data are shown. The monochromatic coloration efficiency (550 nm) is 26 cm^2/C before and after cycling. However, the peak coloration current density dropped from 2.5 mA/cm^2 to 0.85.mA/cm^2 .

The TEM bright field image and accompanying SAD pattern for a typical sol-gel film are shown in Figure 9. There are some micro-crystallites, but this film is mainly amorphous. The diffuse halos in the SAD pattern correspond to the cubic NiO phase. The few spots seen in the diffraction pattern correspond to Silicon that had been added as a standard. Bright field images of the nickel oxide film after cycling are shown in Figure 10. After cycling, the SAD pattern from the film still shows diffuse NiO rings, but there is also a broad diffuse amorphous halo and some scattered spots.

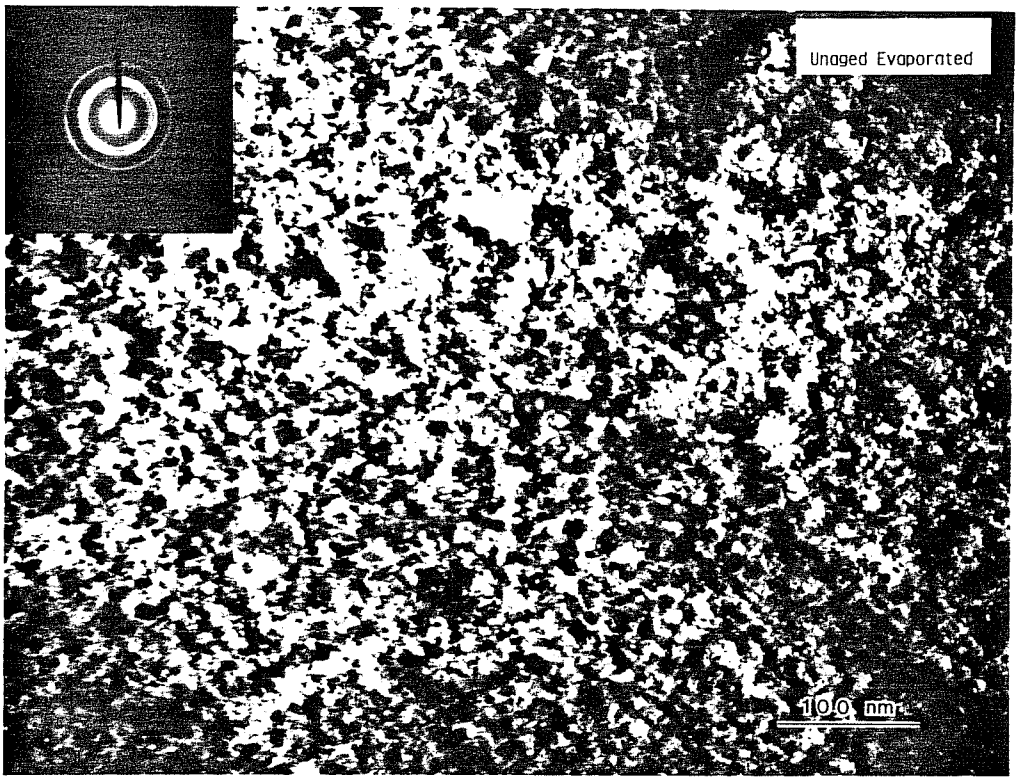

(A)

XBB 889-8519A

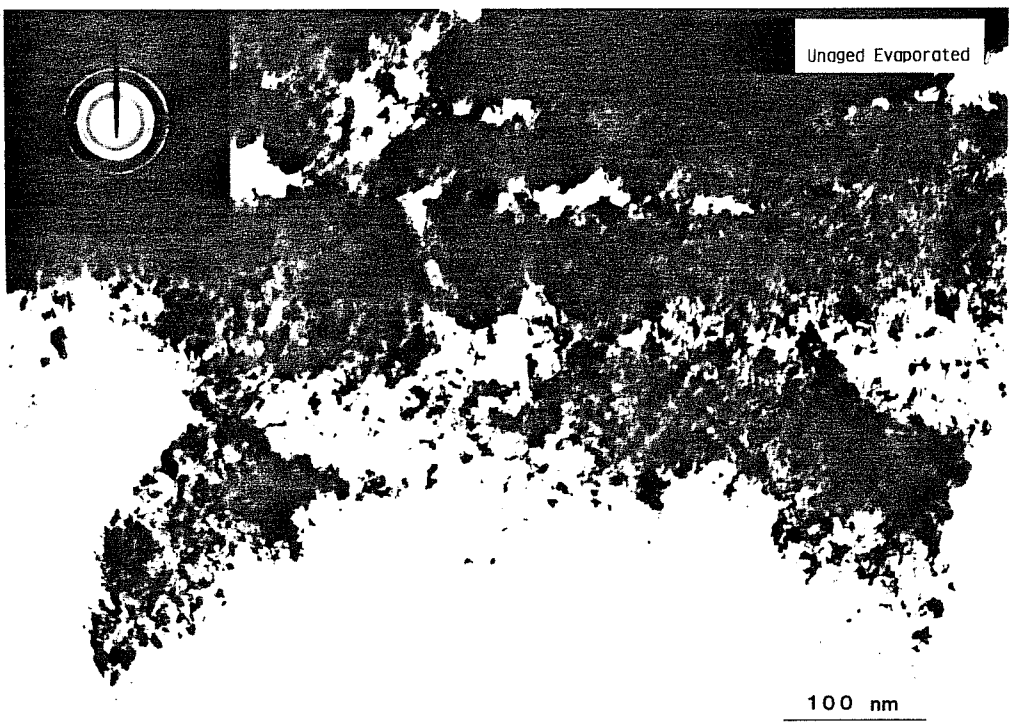

(B)

XBB 889-8518A

Figure 4. Transmission electron micrographs of an uncycled nickel oxide film made by evaporation. The diffraction pattern shows cubic NiO (see inset). Two typical regions are shown as (A) high crystallinity, and (B) lower crystallinity/amorphous region.

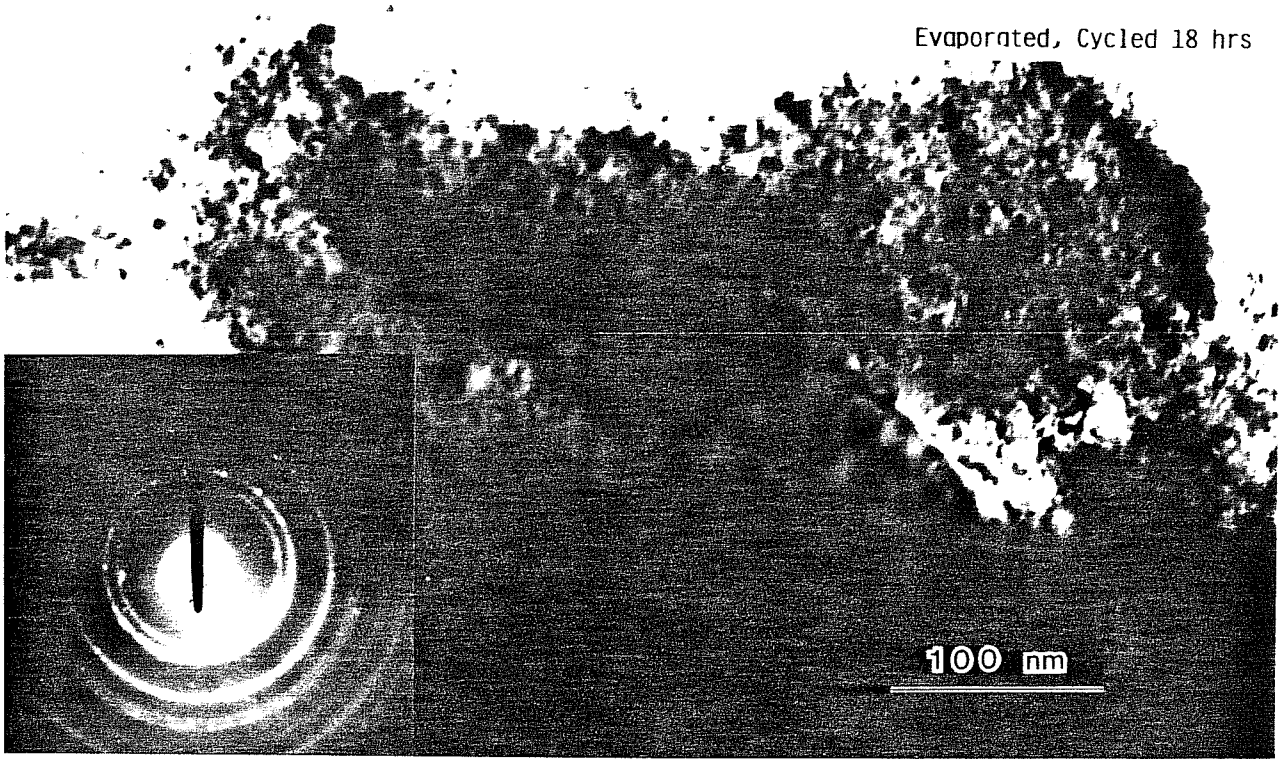

(A)

XBB 897-6202

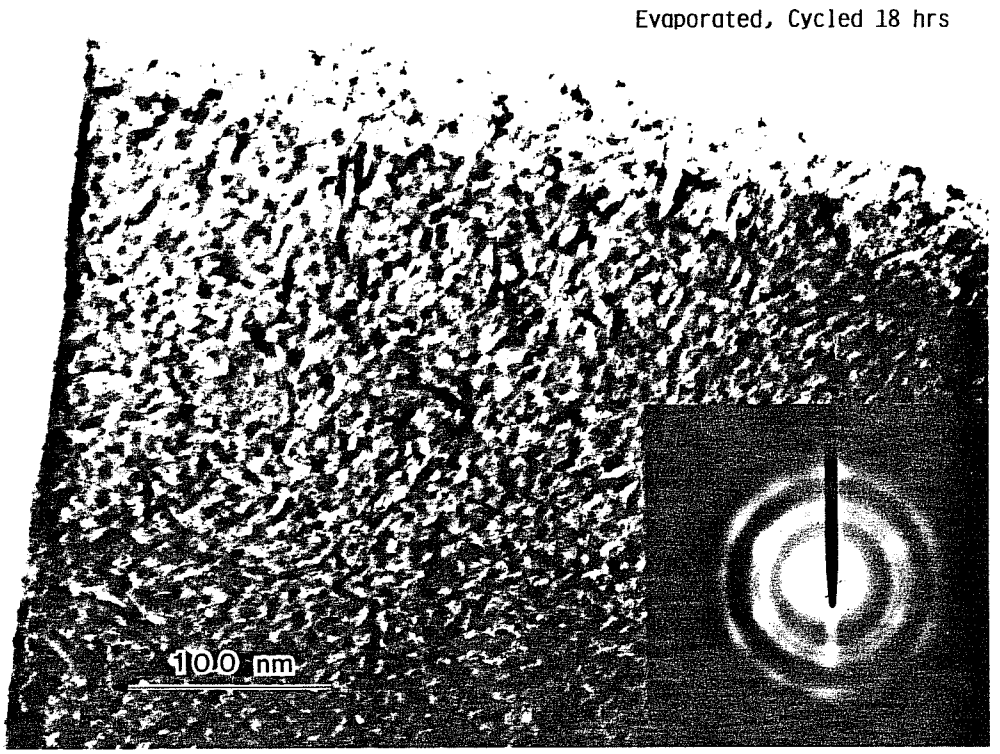

(B)

XBB 897-6199

Figure 5. Transmission electron micrograph of a nickel oxide film made by evaporation after cycling for 18 hours. The diffraction pattern shows cubic NiO (see inset). Two typical regions are shown as (A) high crystallinity, and (B) high crystallinity with some preferential orientation region.

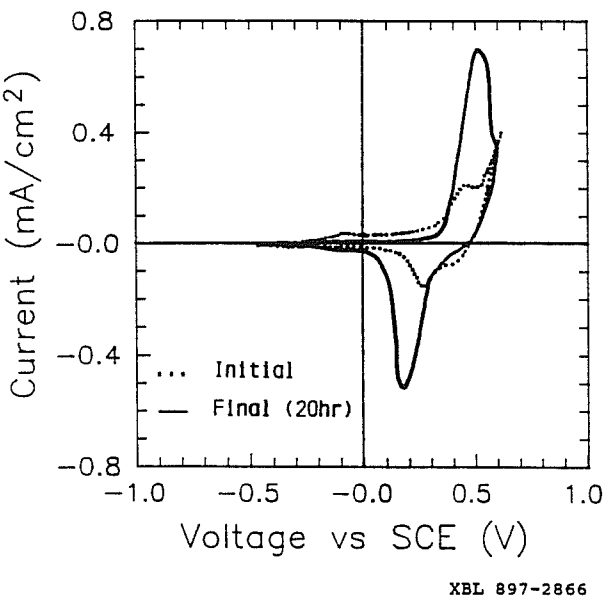

Figure 6. Voltammetry of electrochromic nickel oxide prepared by sol-gel deposition. Shown are cycled and uncycled data. The scan rate is 6 mV/s.

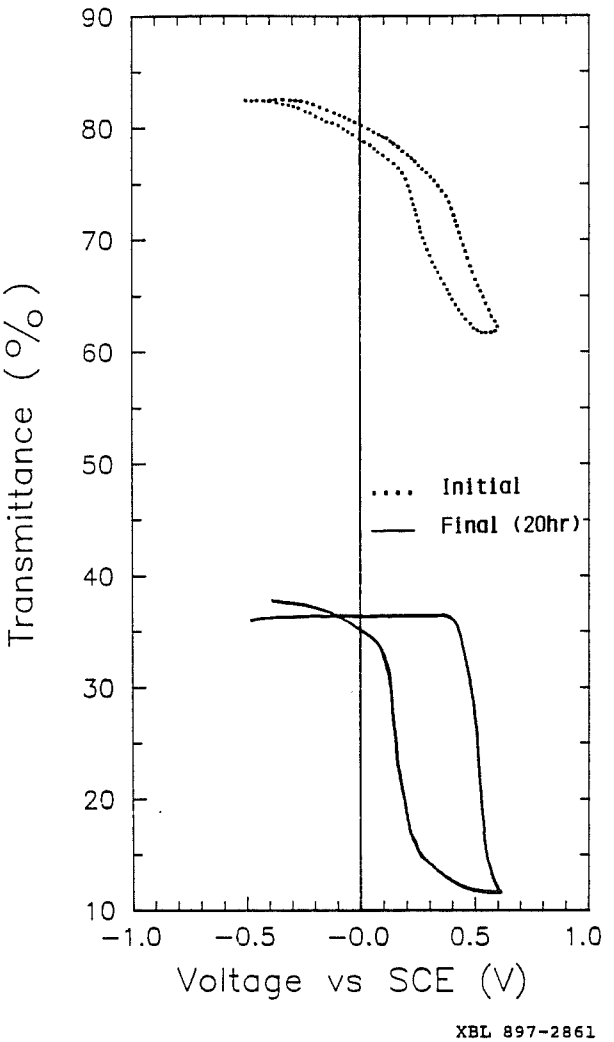

Figure 7. Transmittance (550 nm) versus voltage relationship for electrochromic nickel oxide prepared by sol-gel deposition. Shown are cycled and uncycled data. The scan rate is 6 mV/s.

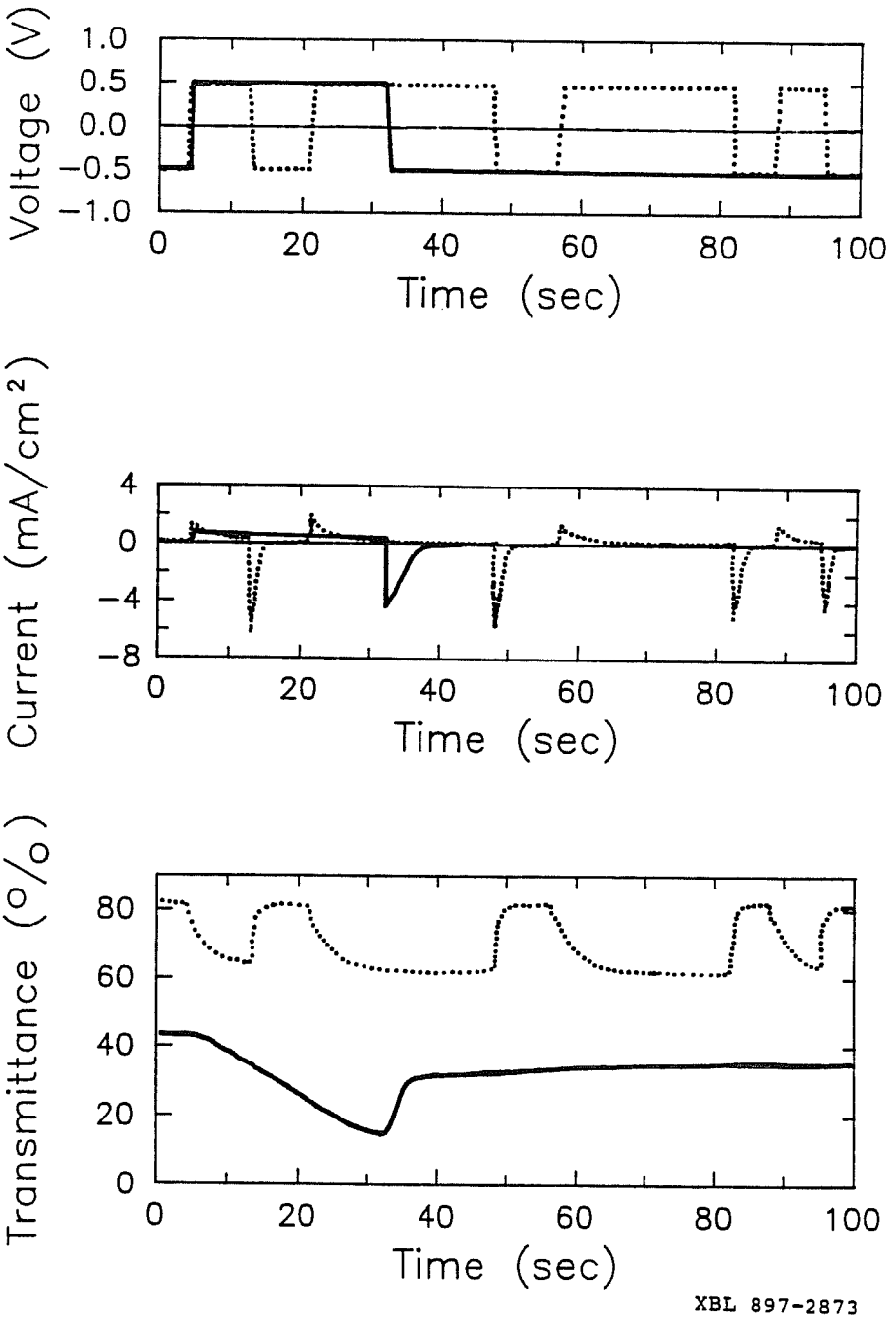

Figure 8. Time-Voltage/Current/Transmittance (550 nm) relationships for a sol-gel prepared electrochromic nickel oxide.

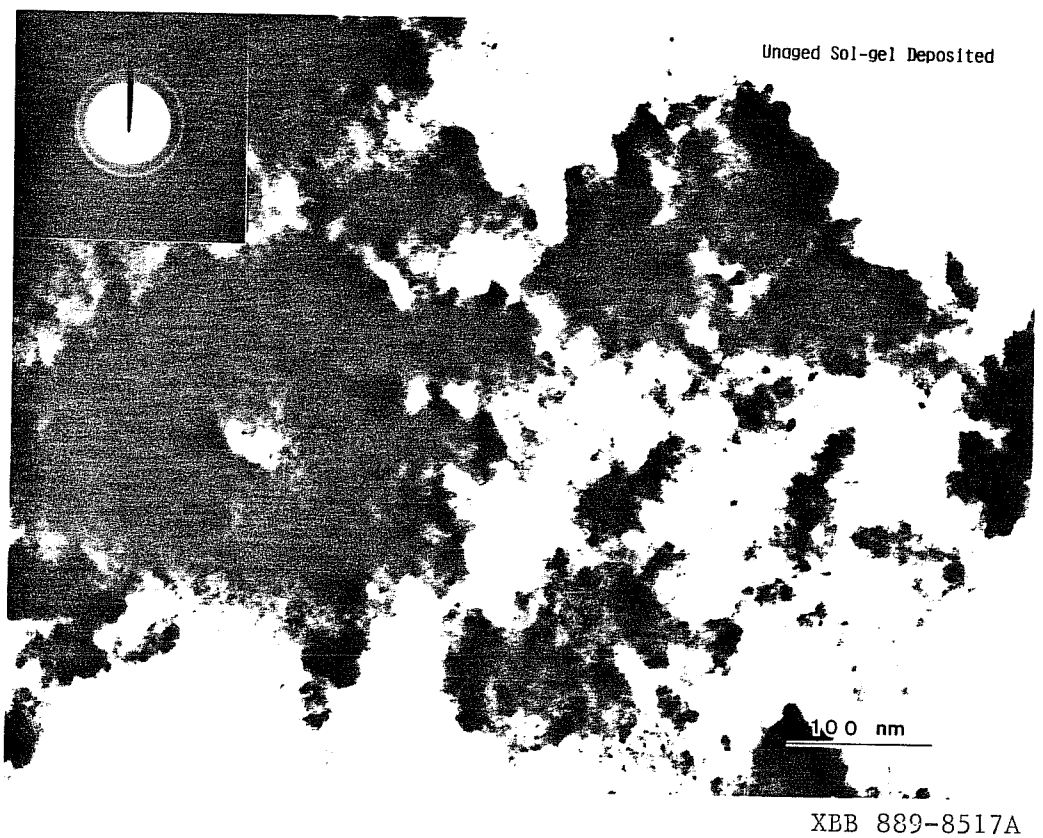

Figure 9. Transmission electron micrograph of a nickel oxide film made by sol-gel. The diffraction pattern shows an amorphous phase with micro-crystalline cubic NiO particles (see inset).

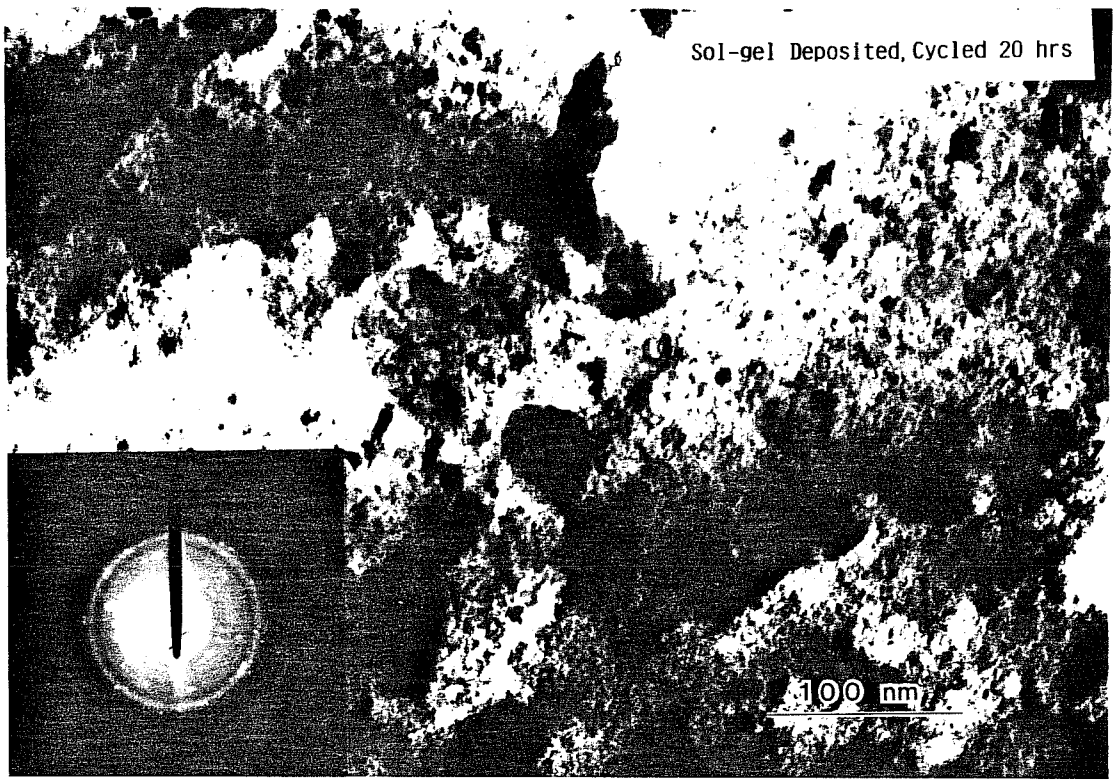

XBB 897-6201

Figure 10. Transmission electron micrograph of a nickel oxide film made by sol-gel after cycling for 20 hours. The diffraction pattern shows an amorphous phase coexisting with crystalline particles.

3.3 Sputtered Films

The characteristic voltammetry (-0.5 to 0.6 V) for a d.c reactively-sputtered film is shown in Figure 11. Both the initial and final characteristics are depicted. The final characteristics are obtained after cycling application of a square wave potential of -0.5 to 0.5 V for 17 hours, covering about 200 cycles. Both the coloration and bleaching peak increase in size after cycling. The coloration peak shifts from about 450 mV to 500 mV, while the bleaching peak shifts from about 250 mV to 200 mV after cycling. A change in transmittance range is noted after cycling, as shown in Figure 12. The bleached to colored transmittance (550 nm) ranges from 60-44% for uncycled films compared to 64-34% for cycled films. This represents a ΔT of 16% changing to 30% after cycling. Also, the transmission in the bleached condition increased by 4%. The characteristic time-voltage/current/transmittance plot for a sputtered film is shown in Figure 13. The monochromatic coloration efficiency (550 nm) is 31 cm^2/C initially and increases to 36 cm^2/C after cycling. This reflects the decline in peak coloration current density from about 3.9 mA/cm^2 to 2.1 mA/cm^2.

The TEM analysis of these films show them to be polycrystalline cubic NiO with an average grain size of 20-30 nm as shown in Figure 14. This contrasts with other TEM studies on the microstructure of nickel oxide coatings made by reactive r.f. sputtering from a nickel target which have shown an average grain size ranging from 7-17 nm.[21]

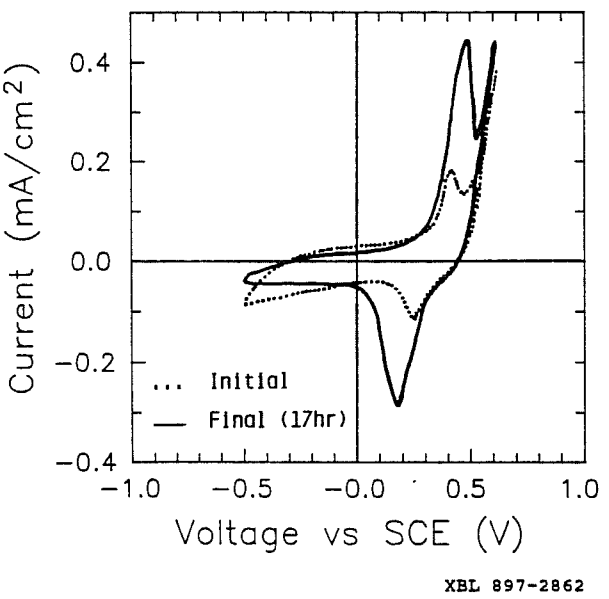

Figure 11. Voltammetry of electrochromic nickel oxide prepared by sputtering. Shown are cycled and uncycled data. The scan rate is 10 mV/s.

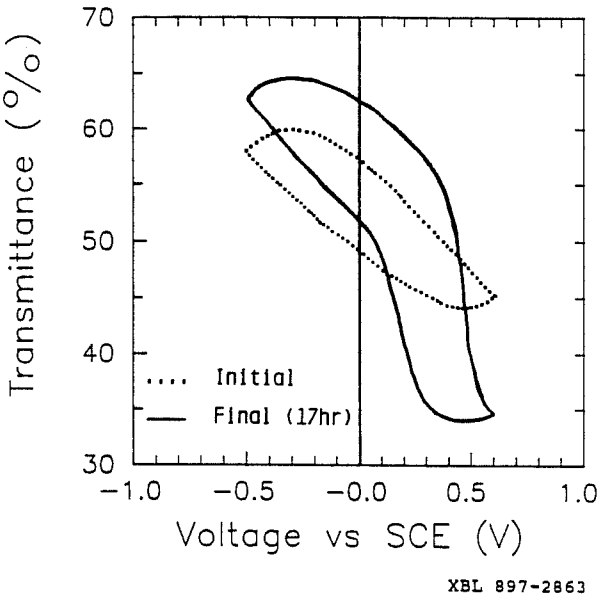

Figure 12. Transmittance (550 nm) versus voltage relationship for electrochromic nickel oxide prepared by sputtering. Shown are cycled and uncycled data. The scan rate is 10 mV/s.

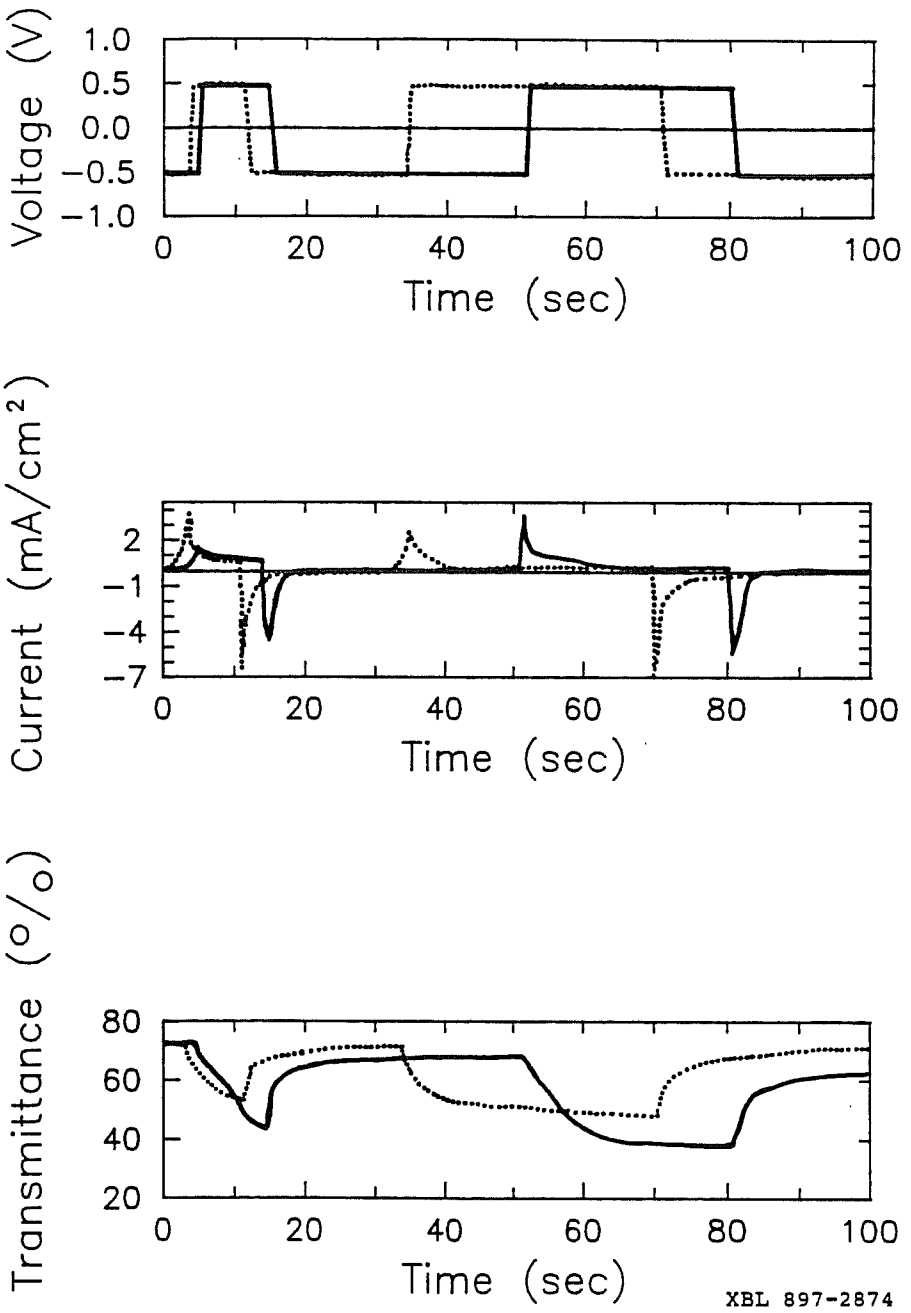

Figure 13. Time-Voltage/Current/Transmittance (550 nm) relationships for sputtered electrochromic nickel oxide.

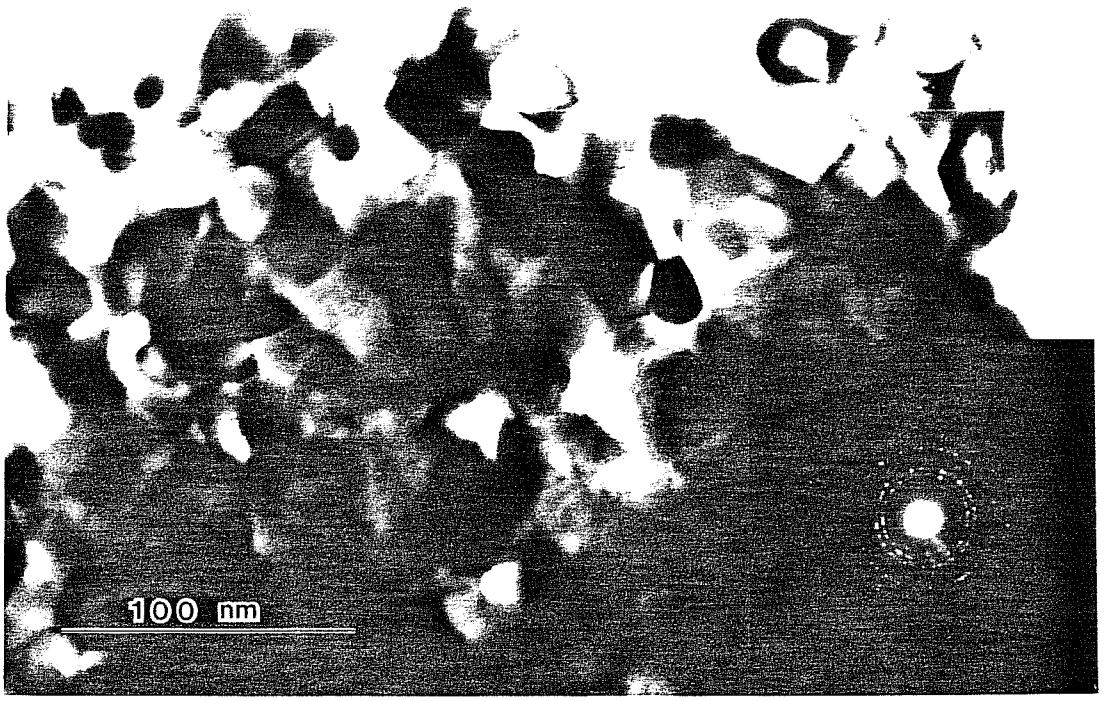

XBB 899-8073

Figure 14. Transmission electron micrograph of a nickel oxide film made by sputtering after cycling for 3 hrs. The diffraction pattern in inset indicates that the film is polycrystalline. From the image the grain size was measured at 20-30 nm.

4. CONCLUSIONS

This study begins to show the variation one can obtain from nickel oxide electrochromic film made by different methods. Of the films investigated, the evaporated and sputtered films showed the highest degree of crystallinity, although their crystallites were very small. All films had some degree of amorphous character with the sol-gel deposited films showing the most. All films had a polycrystalline or microcrystalline phase that corresponded to cubic NiO as best as we could identify it. No other dominant phase was found. These findings support our other studies using ex-situ X-ray Photoelectron spectroscopy and Ion backscattering.[4] There may be chemical differences in each sample which we did not detect, such as Ni or O defect densities, which could alter the coloration and performance of the fims. Films that were cycled for 17-20 hours all tended to have improved transmittance range. The evaporated film went from ΔT (550 nm) of 40% to 60%. For sol-gel films the change went from 20% to 30%. For the sputtered film the change went from 26% to 30%. The sol-gel films showed a large residual coloration in the bleached state after cycling; about a 40% decline was noted. For sputtered films, the films increased their transmittance by about 5% after cycling. Overall, after cycling the films appeared to be slightly more crystalline, but no hydroxide phase was noted. It is possible this phase is only a minor component or is completely amorphous, if it exists at all, under the vacuum conditions of analysis. In all films, after cycling there were increases in the coloration and bleaching peaks. Also, peak

shifts were noted after cycling; the coloration peak tended to shift to higher potentials and the bleaching peak shifted to lower potentials. With the higher number of cycles the changes in each film tended to stabilize. The e-beam evaporated film showed the best electrochromic properties. The sputtered film was the second best in properties. The overall coloration efficiency (550 nm) for these films ranged from 26-36 cm^2/C. In further investigations of the chemistry, structure, and morphology of these film we hope to further explain their relationship to the electrochemical and switching properties of electrochromic nickel oxide.

5. ACKNOWLEDGEMENTS

A special thanks goes to Mr. S. Selkowitz and Prof. J. Washburn for their continued support of this project.

This work was performed at the Lawrence Berkeley Laboratory, under a joint project between the Applied Science Division and the Materials and Chemical Science Division. This work was supported by the Assistant Secretary for Conservation and Renewable Energy, Office of Solar Heat Technologies, Solar Building Division, of the U.S. Department of Energy under Contract No. DE-AC03-76SF00098.

6. REFERENCES

1. C.M. Lampert, "Electrochromic Materials and Devices for Energy Efficient Windows," Solar Energy Materials, 11(1982)1.

2. C.M. Lampert and C.G. Granqvist, eds., Large Area Chromogenics: Materials and Devices for Transmittance Control, Optical Engineering Press, Bellingham, WA, 1990.

3. A. Pennisi and C.M. Lampert, "Optical Properties of Electrochromic Nickel Oxide Devices Utilizing A Polymeric Electrolyte," Solar Energy Materials, to be published 1990, LBL-24024.

4. C.M. Lampert, "Chemical and Optical Studies of Electrochromic Hydrated Nickel Oxide Films and Devices," in Large Area Chromogenics: Materials and Devices for Transmittance Control, C.M. Lampert and C.G. Granqvist, eds., Optical Engineering Press, Bellingham, WA, 1990.

5. R.G. Gunter, ed., Proc. of the Symposium On the Nickel Electrode, The Electrochem. Soc., 82-4(1982)1.

6. T.R. Omstead, P.C. Yu, and C.M. Lampert, "Chemical and Optical Properties of Electrochromic Nickel Oxide Films," Solar Energy Materials, 14 (1986)1.

7. J.S.E.M. Svensson and C.G. Granqvist, Proc. of SPIE, 653(1986)10.

8. J.S.E.M. Svensson and C.G. Granqvist, Appl. Phys. Lett., 49(1986)1566.

9. K. Bange, F.G.K. Baucke, B. Metz, Proc. of SPIE, 1016(1988)170.

10. P.C. Yu, G. Nazri, and C.M. Lampert, "Spectroscopic and Electrochemical Studies of Electrochromic Hydrated Nickel Oxide Films," Solar Energy Materials, 16(1987)1.

11. P.C. Yu and C.M. Lampert, "In-situ Spectroscopic Studies of Electrochromic Switching films for Glazings," Solar Energy Materials, 19 (1989)1.

12. A. Pennisi and F. Simone, Proc. SPIE 1016, (1988)176.

13. M.K. Carpenter, R.S. Conell, and D.A. Corrigan, Solar Energy Materials, 16 (1987)333.

14. M.K. Carpenter and D.A. Corrigan, J. Electrochem. Soc., 136(1989)1022.

15. J. Desilvestro, D.A. Corrigan, and M.J. Weaver, J. Electrochem. Soc., 135(1988)885.

16. D.A. Corrigan and S.L. Knight, J. Electrochem. Soc., 136(1989)613.

17. J. Desilvestro, D.A. Corrigan, and M.J. Weaver, J. Phys. Chem., 90(1986)6408.

18. P. Delichere, S. Joiret, and A. Hugot-Le Goff, Proc. of SPIE, 1016(1988)165.

19. P. Flalaras, A. Hugot Le-Goff, and S. Joiret, "Optical techniques for the study of electrochromic phenomena: application of Raman spectroscopy and optical multichannel ananlysis (OMA) to the coloration of oxides and polymer films," in Large Area Chromogenics: Materials and Devices for Transmittance Control, C.M. Lampert and C.G. Granqvist, eds., Optical Engineering Press, Bellingham, WA, 1990.

20. G. Nazri, D.A. Corrigan, and S.P. Maheswari, Langmuir, 5(1989)17.

21. W. Estrada, A.M. Andersson, and C.G. Granqvist, J. Appl. Phys., 60(1988)3678.